Available online at www.sciencedirect.com
ScienceDirect
ELSEVIER
Dyes and Pigments 77 (2008) 408–414
DYES and PIGMENTS
www.elsevier.com/locate/dyepig

A novel Y-type, two-photon active fluorophore: Synthesis and application in ratiometric fluorescent sensor for fluoride anion

Meng Zhang [a], Manyu Li [b], Fuyou Li [a,*], Yunfei Cheng [a],
Jianping Zhang [b,c], Tao Yi [a,*], Chunhui Huang [a]

[a] Department of Chemistry and Laboratory of Advanced Materials, Fudan University, Shanghai 200433, PR China
[b] State Key Laboratory for Structural Chemistry of Unstable and Stable Species, Institute of Chemistry, Chinese Academy of Sciences, Beijing 100080, PR China
[c] Department of Chemistry, Renmin University of China, Beijing 100872, PR China

Received 16 February 2007; received in revised form 2 July 2007; accepted 6 July 2007
Available online 22 July 2007

Abstract

The detection of fluoride anion (F^-) has recently attracted much attention, because F^- is highly relevant to health and environmental issues. A novel Y-shaped fluorophore with an imidazole ring core, (*E*,*E*′-4,4′-[(2,2′-bis(ethene-2,1-diyl)dibenzoate)-(2-(4-(methoxycarbonyl)phenyl)-1*H*-imidazole-4,5-diyl) (**1**), was synthesized and used as a ratiometric fluorescent sensor for fluoride anion. Upon addition of fluoride anion, the emission color of **1** turned from green to brown under ambient conditions, owing to deprotonation of the imidazole core. Importantly, upon complexation with fluoride anion, an obvious variation in the maximum wavelength of the two-photon excited fluorescence (TPEF peak) was observed from 490 to 565 nm, indicating that **1** is an excellent ratiometric TPEF-sensor for fluoride anion.

Keywords: Two-photon; Ratiometric; Fluorescent sensor; Fluoride anion

---

1. Introduction

The search of a chemosensor for recognition and sensing of anionic analytes is emerging as a research area of considerable importance [1–3]. Among various anions, fluoride ion (F^-) is one of the most significant due to its important role in teeth-protection and bone-growth [4,5]. A number of synthetic chemosensors for this important analyte have been designed by utilizing chromogenic [6–8] and fluorogenic [9–20] behaviors. For most of the reported fluorescent F^-–sensors, the binding of F^- causes a quenching [9–15] or increase [13,16–20] of the fluorescence emission. However, in most practical applications, changes in fluorescence intensity (fluorescence quenching or enhancement) can also be caused by many other variable factors such as photobleaching, concentration of sensor, and the environment around the sensor molecule (pH, polarity, temperature, and so on) [21]. To increase the selectivity and sensitivity of a measurement, ratiometric measurements are utilized. The ratiometric methods using one excitation wavelength and taking the intensity ratio at two different absorption or emission wavelengths can offer intrinsic advantages in both chemical and biological sensing [22–31]. For example, ratiometric fluorescent probes permit signal rationing and thus increase the dynamic range and provide built-in correction for environmental effects. Although a few ratiometric fluorescent sensors for fluoride anion have been reported [11,32–37], the output signal of these sensors is limited to the single-photon related fluorescence.

Two-photon excited fluorescence (TPEF) has recently especially useful application in biological samples [38–41] for its advantages of improvement of depth penetration at low

---

* Corresponding authors.
E-mail address: fyli@fudan.edu.cn (F. Li).

0143-7208/$ - see front matter © 2007 Elsevier Ltd. All rights reserved.
doi:10.1016/j.dyepig.2007.07.003

incident intensity and reducibility of background cellular autofluorescence. Recently, some TPEF fluorophores sensitive to ions and Cys/Hcy have been reported [42–46]. Up to now, only one TPEF system for anion has been reported by our group [47]. We used three organic boron derivatives as TPEF-sensor for fluoride anion. However, the TPEF emissions of all these sensors were quenched upon addition of fluoride anion [47]. As an extension of our previous work on TPEF-sensor [44–47], herein, a novel Y-shaped fluophore **1** (Scheme 1) was designed and synthesized as a ratiometric TPEF sensor for fluoride anion.

2. Experimental

2.1. Materials

Unless otherwise noted, materials were purchased from commercial suppliers and used without further purification. The solutions of Cu^{2+}, Cu^{+}, Hg^{2+}, Fe^{2+}, Mn^{2+}, Na^{+}, K^{+} and Ca^{2+} were prepared from their chloride salts, solutions of Fe^{3+}, Pb^{2+}, Cd^{2+}, Co^{2+}, Ni^{2+}, Cr^{3+}, Ag^{+} and Mg^{2+} were prepared from their nitrate salts, and solution of Zn^{2+} was prepared from Zn(II) acetate. HEPES buffer solutions (pH = 7.2) were prepared using 50 mM HEPES and proper amount of NaOH.

Butane-2,3-dione and 4-formyl-benzoic acid methyl ester were commercially available from Aldrich Chemical Co. Tetrabutylammonium salts (F^-, Cl^-, Br^-, I^-, NO_3^-, ClO_4^-, $H_2PO_4^-$ and AcO^-) were purchased from Lancaster Chemical Co. All others were purchased from Shanghai Chemical reagent Co. Ltd., and used without further purification. Reactions were monitored by TLC on silica gel 60 F_{254}. Column chromatography purifications were performed on silica gel (HG/T2354-92).

2.2. Instrument

NMR spectra were recorded at 400 MHz spectrometer on a Varion Gemin-400. All chemical shifts are reported in the standard δ notation of parts per million. Mass spectra were recorded with a MA1212 mass spectroscope. Electrospray ionization mass spectra (ESI-MS) were measured on a Micromass LCTTM system. Element analyses were performed on a Vari-oEL III O-Element Analyzer system. UV–vis absorption spectra were conducted on a Shimadzu 3000 spectrophotometer. Fluorescence spectra were measured on an Edinburgh LFS920 luminescence spectrometer with 1000 W xenon lamp. Samples for absorption and emission measurements were contained in 1-cm × 1-cm quartz cuvettes.

2.3. Determination of fluorescent quantum yield

Fluorescence quantum yields Φ were measured by using fluorescein ($\Phi_F = 0.93$ in ethanol) as a reference, which are calculated using the following equation [48–50].

$$\Phi_{sam} = \Phi_{ref}\left[\frac{I_{sam}}{I_{ref}}\right]\left[\frac{A_{ref}}{A_{sam}}\right]\left[\frac{n_{sam}}{n_{ref}}\right]^2$$

Φ_{sam} and Φ_{ref} stand for the fluorescent quantum yield of the sample and the reference, respectively; I_{sam} and I_{ref} stand for the integrated emission intensity of the sample and the reference, respectively; A_{sam} and A_{ref} stand for the absorbance of the sample and the reference, respectively. n_{sam} and n_{ref} stand for the refractive index of the sample and the reference, respectively.

2.4. Determination of two-photon absorption cross-section (σ)

Two-photon absorption (TPA) cross-sections (σ) were determined by the method of two-photon induced fluorescence using Rhodamine B as a reference with known two-photon absorption cross-sections. A regenerative amplifier (Spitfire, Spectra Physics) which was seeded by a mode-locked Ti:Sapphire laser (Tsunami, Spectra Physics) produced laser beam centered at 795 nm and pulse width of about 120 fs. The laser was used to drive an optical parameter amplifier (OPA-800CF, Spectra Physics) and delivered our desired wavelength range of 650–800 nm. It was focused into a quartz cuvette with an optical path length of 25 mm. The two-photon induced fluorescence was collected and sent to a polychromator (Spectropro-550i, Acton) equipped with a liquid-nitrogen-cooled CCD detector (SPEC-10-400B/LbN, Roper Scientific). To reject an interference of stray laser light, a 10-mm long saturated aqueous solution of $CuSO_4$ was placed in front of the entrance slit. Compound **1** was dissolved in acetonitrile at a concentration of 10^{-4} M and Rhodamine B in ethanol at the same

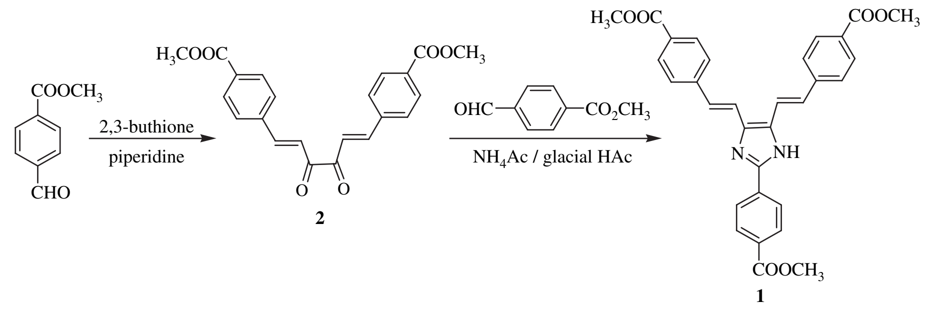

Scheme 1. Synthetic route of **1**.

concentration. TPEF cross-section (σ') and TPA cross-section (σ) were measured on the basis of the following expression [51].

$$\sigma'_{\mathrm{sam}} = \sigma'_{\mathrm{ref}} \frac{C_{\mathrm{ref}}}{C_{\mathrm{sam}}} \frac{n_{\mathrm{ref}}}{n_{\mathrm{sam}}} \frac{F_{\mathrm{sam}}}{F_{\mathrm{ref}}}$$

$$\sigma_{\mathrm{sam}} = \frac{\sigma'_{\mathrm{sam}}}{\Phi_{\mathrm{sam}}}$$

where σ'_{sam} and σ'_{ref} stand for the two-photon excited fluorescence cross-section of the sample and the reference, respectively; C_{sam} and C_{ref} stand for the concentration of the sample and the reference, respectively; n_{sam} and n_{ref} stand for the refractive index of the solvents of the sample and the reference, respectively; F_{sam} and F_{ref} stand for the intensity of two-photon induced fluorescence of the sample and the reference, respectively; σ_{sam} and Φ_{sam} stand for the two-photon absorption cross-section and fluorescent quantum yield of the sample, respectively.

2.5. Calculations of binding constants

Binding constant K of 1:1 compound/F$^-$ complex formation calculated by the UV–vis absorption method is obtained by the following equation [52].

$$A = A_0 + \frac{A_{\mathrm{lim}} - A_0}{2C_0} \left\{ C_{\mathrm{H}} + C_{\mathrm{G}}/K - \left[(C_{\mathrm{H}} + C_{\mathrm{G}} + 1/K)^2 - 4C_{\mathrm{H}}C_{\mathrm{G}} \right]^{1/2} \right\}$$

where A represents the ultraviolet absorbance; A_0 represents the absorbance of pure host; C_{H} and C_{G} are the corresponding concentration of host and cation guest; c_0 represents the concentration of pure host; K is the binding constant.

2.6. Anion titration of *1*

Spectrophotometric titrations were performed on the CH_3CN solutions of **1** (10 μM). Typically, aliquots of fresh anions (F^-, Cl^-, Br^-, I^-, ClO_4^-, NO_3^-, AcO^-, $H_2PO_4^-$) were added, and the UV–vis absorption and fluorescent spectra of the samples were recorded.

2.7. Synthesis

2.7.1. Dimethyl 4,4′-((1E,5E)-3,4-dioxohexa-1,5-diene-1,6-diyl) dibenzoate (*2*)

The intermediate **2** was prepared according to the literature [53]. Butane-2,3-dione (1.5 mL) was added to the methanol solution of 4-formyl-benzoic acid methyl ester (1.5 mmol) with a drop of piperidine as catalyst. The mixture was refluxed for 6 h under nitrogen atmosphere. After cooling, the precipitate was filtrated and washed with methanol for several times, and yellow powder was obtained in 24% yield.

2.7.2. (E,E′)-4,4′-[(2,2′-bis(Ethene-2,1-diyl)dibenzoate)-(2-(4-(methoxycarbonyl)phenyl)-1H-imidazole-4,5-diyl) (*1*)

A three-necked round bottomed flask was charged with **2** (1.5 mmol) and ammonium acetate (15 mmol) in glacial acetic acid (25 mL). The reaction mixture was stirred under nitrogen atmosphere for 30 min, then 4-formyl-benzoic acid methyl ester (1.5 mmol) was added dropwise over 1 h with an pressure equalizing funnel. The reaction mixture was heated at 90 °C till TLC monitoring indicated complete consumption of **2**. The resulting solution was cooled to room temperature and poured into 100 mL of ice water, neutralized by ammonia water, and a large amount of residues were emerged. The precipitate was filtered and washed several times by water. Purification by column chromatography using chloroform/petroleum ether as eluent, and then recrystallization in chloroform solution provided green-yellow powder **1** with a yield of 61%. M.P. 177–179 °C; ^{1}HNMR (400 Hz, DMSO-d_6): δ 12.83 (s, NH, 1H), 8.26 (d, $J = 8.2$ Hz, C_6H_5, 2H), 8.10 (d, $J = 8.0$ Hz, C_6H_5, 3H), 7.95(s, C_6H_5, 4H), 7.83 (m, C_6H_5, 3H), 7.79 (s, 2CH, 2H), 7.38 (s, 2CH, 2H), 3.88 (s, OCH_3, 3H), 3.86 (s, $2OCH_3$, 6H); ^{13}CNMR (100 Hz, DMSO-d_6): 52.4, 52.6, 117.9, 122.3, 126.3, 126.7, 126.9, 127.1, 129.9, 130.1, 134.1, 140.6, 142.5, 142.8, 147.2, 166.3, 166.4; ESI-MS: *m/z* (%) 522 (100). Anal. Calcd. for $C_{31}H_{26}N_2O_6$: C, 71.16; H, 4.90; N, 5.59. Found: C, 71.25; H, 5.02; N, 5.36.

3. Results and discussion

3.1. Photophysical properties of *1*

The data of the photophysical properties of **1** are summarized in Table 1. Compound **1** exhibits an intense single-photon absorption (SPA) band centered at 390 nm, corresponding to molar absorption coefficient (ε) of 3.8×10^5 M^{-1} cm^{-1}, which is attributed to the π–π* transition of the conjugation system of **1**. Moreover, the solution of **1** in CH_3CN shows an intense fluorescent emission peaked at 490 nm, with a fluorescent quantum yield of 0.54.

3.2. Single-photon related spectra titration of *1* with fluoride anion

The complexation ability of **1** with fluoride anion was investigated in CH_3CN by UV–vis absorption technology. Fig. 1 shows the absorption response of **1** to n-Bu_4NF (TBAF). Herein, we denoted the mixture of **1** and fluoride

Table 1
Single- and two-photon properties of **1** and **1F** in MeCN

	$\lambda_{\max}^{\mathrm{abs}}$ (nm)	ε (M^{-1} cm^{-1})	λ_{SPEF}[a] (nm)	λ_{TPEF} (nm)	Φ[b]	σ[c] (GM)
1	390	383 000	485	490	0.54	1764
1F	455	447 000	590	565	0.40	1504

[a] Emission maximum wavelength excited at the absorption maximum.

[b] Fluorescence quantum yields in CH_3CN using fluorescein as a standard.

[c] TPA cross-section maxima were measured by the comparative TPEF methods.

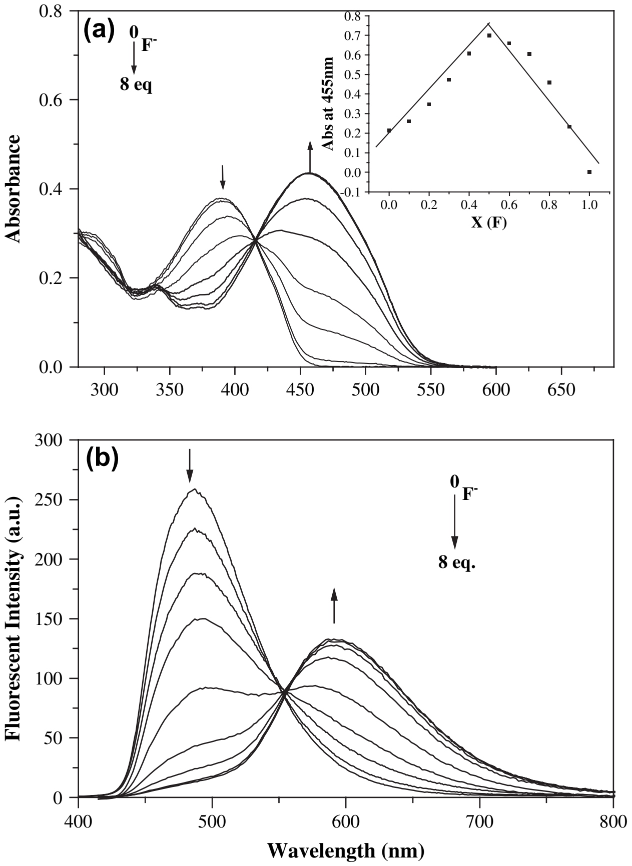

Fig. 1. Change in UV–vis absorption (a) and emission (b) spectra of **1** (10 μM) upon addition of F$^-$ (0–8 equiv) in the CH$_3$CN solution ($\lambda_{ex} = 415$ nm). Inset: Job's plot of the complexation between **1** and F$^-$, total concentration of **1** and F$^-$ was kept constant at 10 μM in MeCN.

anion as complex **1F**. Upon addition of fluoride anion, the band at 390 nm gradually disappeared and a red-shifted absorption band centered at 455 nm increased with a distinct isosbestic point at 415 nm (Fig. 1a), corresponding to a dramatic color change from weak green to yellow (Fig. 2a), which was observed by the naked-eye. This fact implied an obvious interaction between **1** and F$^-$. Job's plot analysis (Fig. 1a inset) showed that the binding stoichiometry for **IF** was 1:1 in CH$_3$CN solution.

Fluorescence titration of **1** with fluoride anion is shown in Fig. 1b. Upon addition of fluoride anion, the stronger fluorescent emission peaked at 485 nm of **1** decreased progressively and a new fluorescent emission band centered at 590 nm appeared, corresponding to a distinct isosbestic point of 554 nm (Fig. 1b). An emission red-shift of 100 nm occurred with this anion-binding event, corresponding to an apparent emission color change from shamrock to brown (Fig. 2b). Furthermore, the fluorescence quantum yields of **1** and **1F** were measured to be 0.54 and 0.40, respectively, suggesting that **1** could be acted as an ideal ratiometric fluorescent chemosensor for fluoride anion.

*3.3. Two-photon related spectra titration of **1** with fluoride anion*

Furthermore, two-photon excited fluorescence (TPEF) measurement was performed in CH$_3$CN solution for **1** (0.1 mM) in the absence or presence of the fluoride anion. TPA cross-section σ and TPEF emission cross-section values ($\sigma\Phi$) were obtained in comparison of that of Rhodamine B [51]. Compound **1** exhibits a broad two-photon absorption band in the range of 650–800 nm. As shown in Fig. 3, the TPA cross-section maximum of **1** was calculated to be 1764 GM (1 GM = 10^{-50} cm^4 s photo^{-1}) at 691 nm. We noted that half the wavelength of the TPA maximum occurred at less than the single-photon maximum wavelength, indicating that there was significant excitonic coupling between the dipolar branches [54]. Furthermore, **1F** also exhibited intense TPEF with a maximal TPA cross-section of 1504 GM. As shown in Fig. 3, the TPEF peaks for **1** and **1F** were at 490 and 565 nm, respectively, which were similar to those of SPEF, indicating that similar mechanisms were involved in both single- and two-photon excited fluorescence. These results indicated that **1** could beserved as an excellent ratiometric TPEF sensor for fluoride anion.

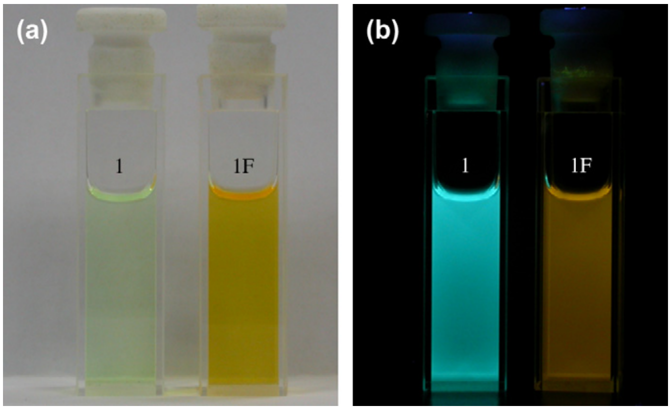

Fig. 2. Color (a) and emission photons (b) (irradiation at 365 nm with UV lamp) of **1** (10 μM) in the absence and presence of 8-fold fluoride anion.

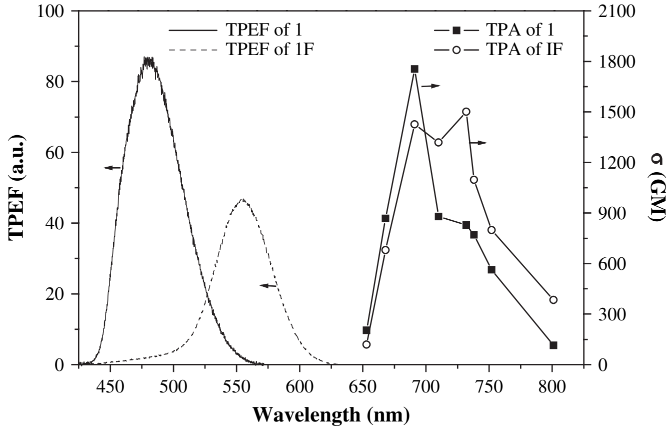

Fig. 3. Two-photon related absorption and fluorescence spectra of **1** (0.1 mM) and **1F** (the mixture of 0.1 mM **1** and 0.8 mM fluoride anion) in acetonitrile.

3.4. The mechanism of **1** in sensing fluoride anion

To understand the mechanism of **1** in sensing fluoride anion, the Bronsted acid–base reaction between **1** and F^- was performed. When strong bases such as Bu_4NOH and NaH were added into the solution of **1**, obviously spectral red-shifts of the absorption and emission bands of **1** were observed (Fig. 4), which was similar to those of **1** with fluoride anion. However, upon addition of weak organic base NEt_3, no obvious changes were observed, which revealed that the reaction between F^- and the NH bond of imidazole group of **1** was a deprotonation process and not hydrogen bonding effect. The deprotonation mechanism of imidazole core by fluoride anion was also confirmed by ^1H NMR titration (Fig. 5). When fluoride anion (dissolved in DMSO-d_6) was added into DMSO-d_6 solution of **1**, a little downfield shift of the imidazole NH proton (12.83 ppm) broadened and then finally disappeared. Similar observation was also reported in the other fluoride sensors with amide (NH) group as receptor [16,32].

The fluorophore **1** is a Y-shaped molecule based on an electron-withdrawing imidazole core (A) connected with three branches of electron-withdrawing group (A′: $-COOCH_3$) via two different conjugated bridges, ethenylphenyl (π_1) and phenyl (π_2) (see Scheme 2). And strong intramolecular charge transfer (ICT) of A′–π_1–A–π_1–A′ and/or A′–π_1–A–π_2–A′ structure caused the obvious absorption and fluorescent emission of **1**. Upon addition of fluoride anion, the imidazole core of **1** was deprotonated and the core became an electron donor. Then, the system switched to an intramolecular charge transfer of A′–π–D (A′: $-CO_2CH_3$, D: imidazole anion core) from that of A′–π–A (A′: $-CO_2CH_3$, A: imidazole core) (see Scheme 2), and the variation of intermolecular proton transfer (IPT) to intramolecular charge transfer (ICT) could be observed for **1**. As a result, the absorption and emission modification and corresponding color change were observed upon addition of fluoride anion.

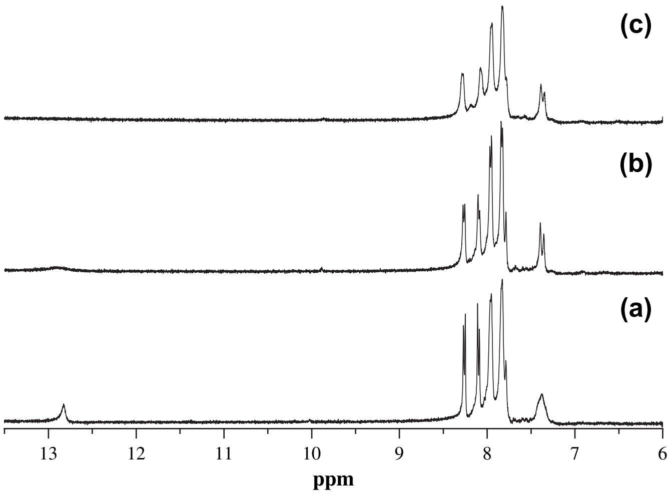

Fig. 5. Partial ^1H NMR spectra of **1** (1.15×10^{-2} M) in DMSO-d_6 in the absence (a) and presence of 1 equiv (b) and 8 equiv (c) fluoride anion. Each ^1H NMR spectrum is measured after 2 min upon addition of fluoride anion.

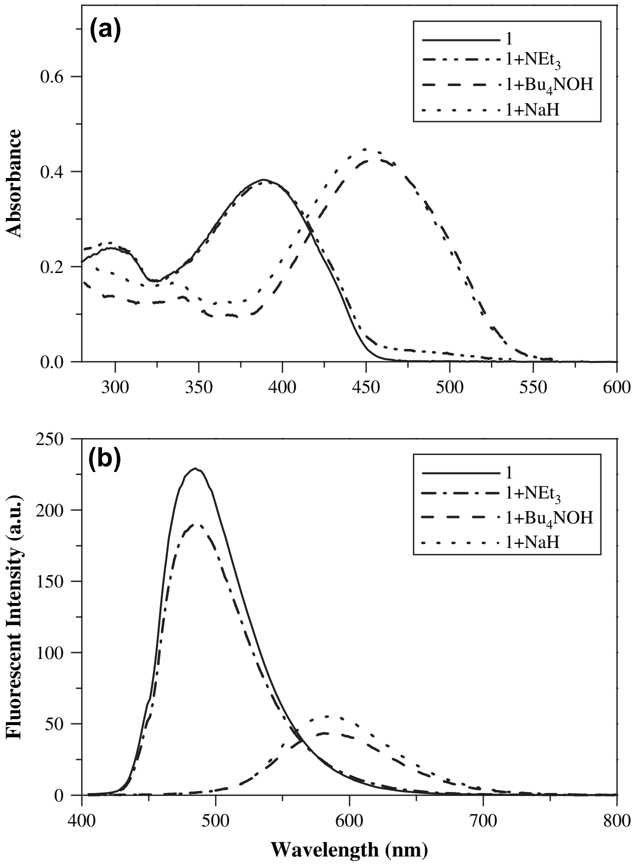

Fig. 4. Absorption (a) and fluorescent emission (b) spectra of **1** (10 μM) upon addition of Bu_4NOH, NaH and NEt_3 (100 μM), respectively. $\lambda_{ex} = 415$ nm.

3.5. Spectral titration of **1** with other anions

For an excellent chemosensor, high selectivity is a matter of necessity. Herein, the selective complexation studies of **1** by absorption and fluorescent titration experiments were then

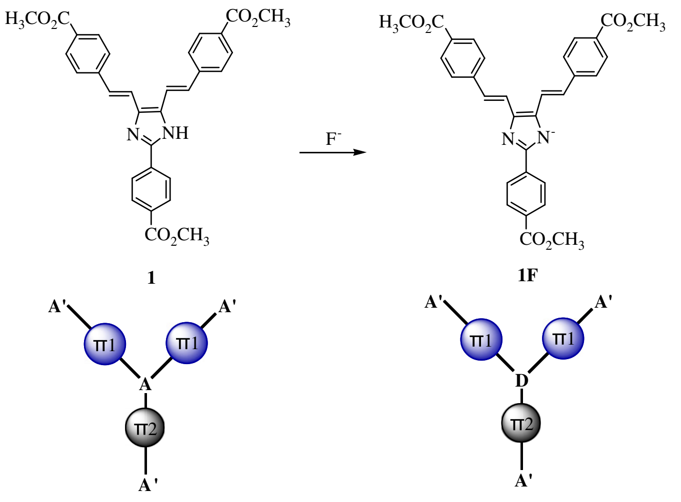

Scheme 2. The sensing mechanism of **1** with fluoride anion.

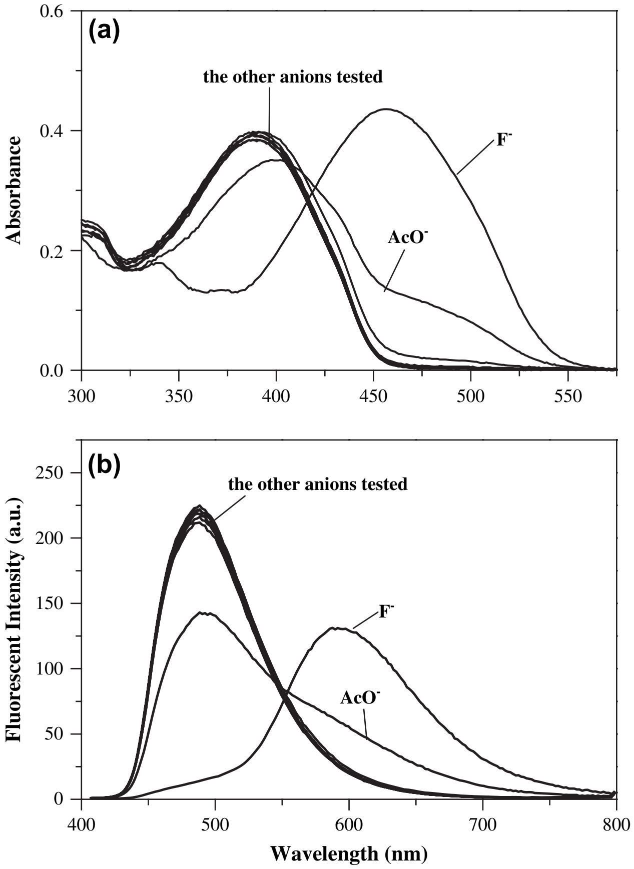

Fig. 6. Absorption (a) and fluorescence (b) spectra of **1** (10 μM) in MeCN solution after the addition of 80 μM Cl^-, Br^-, I^-, NO_3^-, ClO_4^- and $H_2PO_4^-$ ion.

extended to related anions in CH_3CN solution. Fig. 6 shows the absorption and fluorescent spectra of **1** (10 μM) in CH_3CN solution after the addition of 80 μM of various anions. Interestingly, **1** shows a weak complexation with AcO^- and scarcely any response with Cl^-, Br^-, I^-, NO_3^-, ClO_4^- or $H_2PO_4^-$. The K values for the binding effect of **1** with F^- and AcO^- are 7.3×10^3 and 3.5×10^3, respectively. For other anions, such as Cl^-, Br^-, I^-, NO_3^-, ClO_4^-, the absorption titration changes were not obvious enough to calculate the corresponding K values.

Furthermore, by using the ratio (R) of fluorescence intensity at 590 and 485 nm as output signal, the representative recognizing behavior of **1** toward anions in CH_3CN solution is shown in Fig. 7. Upon addition of 8-fold anions, very mild change of **1** was observed for AcO^- (3.6-fold), while Cl^-, Br^-, I^-, NO_3^-, ClO_4^- and $H_2PO_4^-$ showed very weak response (Fig. 7). Only the addition of F^- resulted in a prominent variation (81-fold) of the ratio (***R***) of fluorescence emission intensity at 590 and 485 nm, which indicated the high selectivity of **1** to F^-. As shown in Fig. 7, the competition experiment was also carried out by adding F^- to the solution of **1** in the presence of other anions. No significant variation in fluorescent intensity was found by comparison with that containing only fluoride anion. The results indicate that the sensing of F^- by **1** is hardly affected by these commonly coexistent anions.

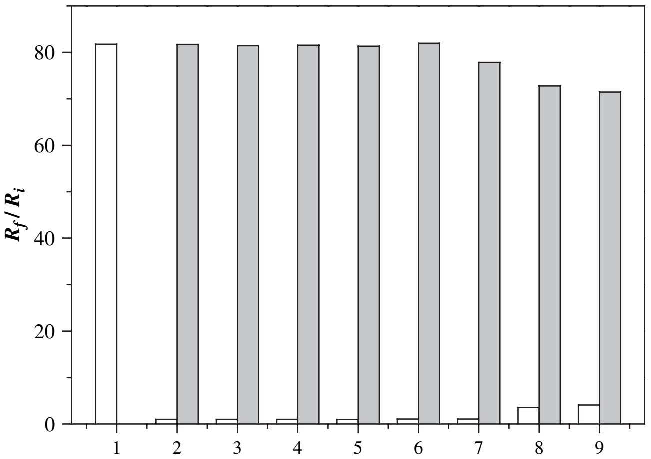

Fig. 7. Fluorescent responses of **1** (10 μM) in the presence of various anions (8 equiv) in MeCN solution. Bars represent the final ratio (R_f) of fluorescence intensity at 590 and 485 nm over the initial ratio (R_i) of fluorescence intensity at 590 and 485 nm. White bars represent the addition of 8-fold various anions to a 10 μM solution of **1**. Gray bars represent the addition of fluoride anion (80 μM) to the above solution, respectively. ($\lambda_{ex} = 415$ nm). (1) F^-; (2) Cl^-; (3) Br^-; (4) I^-; (5) NO_3^-; (6) ClO_4^-; (7) $H_2PO_4^-$; (8) AcO^-; (9) all other anions except F^-.

4. Conclusions

In summary, we have described a novel Y-shaped imidazole derivative as single- and two-photon excited fluorescent chemosensor for fluoride anion with high selectivity, as well as with ratiometric method. Upon addition of fluoride anion, **1** shows an obvious change in emission color from shamrock to brown at ambient condition, which is due to the deprotonation of the imidiazole core of **1**. Importantly, an obvious variation of TPEF peak from 490 to 565 nm was observed for **1** upon complexation with fluoride anion over the other anions, indicating that **1** can be adopted as an ideal ratiometric TPEF sensor for fluoride anion. The design strategy and remarkable photophysical properties of the sensor would help to extend the development of ratiometric fluorescent sensors for fluoride anion.

Acknowledgments

The authors thank NSFC of China (20490210, 20501006), National High Technology Program of China (2006AA03 Z318), Huo Yingdong Education Foundation (104012) and Shanghai Sci. Tech. Comm. (05DJ14004 and 06QH14002) for financial support.

References

[1] Bianchi A, James KB, Garcia-EspanÄa E, editors. Supramolecular chemistry of anions. New York: Wiley-VCH; 1997.
[2] Martinez-Manez R, Sancenon F. Chem Rev 2003;103:4419.
[3] Schmidtchen FP, Berger M. Chem Rev 1997;97:1609.
[4] Kirk KL. Biochemistry of the halogens and inorganic halides. New York: Plenum Press; 1991. p. 58.
[5] Riggs BL. Bone and mineral research. Amsterdam: Elsevier; 1984. Annual 2, p. 366.

[6] Zhou ZG, Yang H, Shi M, Xiao SZ, Li FY, Yi T, et al. Chem Phys Chem 2007;8:1289.
[7] Zhou ZG, Xiao SZ, Xu J, Liu ZQ, Shi M, Li FY, et al. Org Lett 2006;8:3911.
[8] Xu S, Tian H. J Mater Chem 2005;15:2676.
[9] Kim SK, Yoon J. Chem Commun 2002;770.
[10] Zhang DQ, Shi M, Liu ZQ, Li FY, Yi T, Huang CH. Eur J Inorg Chem 2006;2277.
[11] Lee SH, Kim HJ, Lee YO, Vicensb J, Kima JS. Tetrahedron Lett 2006;47:4373.
[12] Zhou G, Cheng Y, Wang L, Jing X, Wang F. Macromolecules 2005;38:2148.
[13] Arimori S, Davidson MG, Fyles TM, Hibbert TG, James TD, Kociok-Köhn GI. Chem Commun 2004;1640.
[14] Matsunaga H, Kanno C, Yamada H, Takahashi Y, Suzuki TM. Talanta 2006;68:1000.
[15] Sathish RS, Sujith U, Rao GN, Janardhana C. Spectrochim Acta Part A 2006;65:565.
[16] Lu H, Xu W, Zhang D, Chen C, Zhu D. Org Lett 2005;7:4629.
[17] Swamy KMK, Lee YJ, Lee HN, Chun J, Kim Y, Kim SJ, et al. J Org Chem 2006;71:8626.
[18] Xu G, Tarr MA. Chem Commun 2004;1050.
[19] Otón F, Tárraga A, Velasco MD, Espinosa A, Molina P. Chem Commun 2004;1658.
[20] Lin Z, Ou S, Duan C, Zhang B, Bai Z. Chem Commun 2006;624.
[21] Lakowicz JR. Principles of fluorescence spectroscopy. New York: Kluwer; 1999.
[22] Kubo Y, Yamamoto M, Ikeda M, Takeuchi M, Shinkai S, Yamaguchi S, et al. Angew Chem Int Ed 2003;42:2036–40.
[23] Raker J, Glass TE. J Org Chem 2002;67:6113–6.
[24] Fu H, Loo BH, Xiao D, Xie R, Ji X, Yao J, et al. Angew Chem Int Ed 2002;41:962–5.
[25] Cheng YF, Zhao DT, Zhang M, Liu ZQ, Zhou YF, Shu TM, et al. Tetrahedron Lett 2006;47:6413.
[26] Mello JV, Finney NS. Angew Chem Int Ed 2001;40:1536.
[27] Takakusa H, Kikuchi K, Urano Y, Sakamoto S, Yamaguchi K, Nagano T. J Am Chem. Soc 2002;124:1653.
[28] Choi K, Hamilton AD. Angew Chem Int Ed 2001;40:3912.
[29] Xu Z, Qian X, Cui J. Org Lett 2005;7:3029.
[30] Liu B, Tian H. Chem Commun 2005;3156.
[31] Xu ZC, Xiao Y, Qian YH, Cui JN, Cui DW. Org Lett 2005;7:889.
[32] Liu B, Tian H. J Mater Chem 2005;15:2681.
[33] Coskun A, Akkaya E. Tetrahedron Lett 2004;45:4947.
[34] Chen QY, Chen CF. Tetrahedron Lett 2004;45:6493.
[35] Zhao Y, Zhang B, Duan C, Lin Z, Meng Q. New J Chem 2006;30:1207.
[36] Badr IHA, Meyerhoff ME. J Am Chem Soc 2005;127:5318.
[37] Liu B, Tian H. Chem Lett 2005;34:686.
[38] Denk W, Strickler JH, Webb WW. Science 1990;248:73.
[39] Köhler RH, Cao J, Zipfel WR, Webb WW, Hansen MR. Science 1997;276:2039.
[40] Marder SR. Chem Commun 2006;131.
[41] Kim HM, Jeong MY, Ahn HC, Jeon SJ, Cho BR. J Org Chem 2004;69:5749.
[42] Pond SJK, Tsutsumi O, Rumi M, Kwon O, Zojer E, Brédas JL, et al. J Am Chem Soc 2004;126:9291.
[43] Bozio R, Cecchetto E, Fabbrini G, Ferrante C, Maggini M, Menna E, et al. J Phys Chem A 2006;110:6459.
[44] Zhang M, Yu MX, Zhu MW, Li MY, Gao YH, Li L, et al. J Am Chem Soc 2007;129:10322.
[45] Zhang M, Li MY, Zhao Q, Li FY, Zhang DQ, Zhang JP, et al. Tetrahedron Lett 2007;48:2329.
[46] Zhang M, Gao YH, Li MY, Yu MX, Li FY, Li L, et al. Tetrahedron Lett 2007;48:3709.
[47] Liu ZQ, Shi M, Li FY, Fang Q, Chen ZH, Yi T, et al. Org Lett 2005;7:5481.
[48] Demas JN, Crosby GA. J Phys Chem 1971;75:991.
[49] Eaton DF. In: Scaiano JC, editor. CRC handbook of organic photochemistry I. Boca Raton, FL: CRC Press; 1989.
[50] Selvi S, Pu SC, Cheng YM, Fang JM, Chou PT. J Org Chem 2004;20:6674.
[51] Xu C, Webb WW. J Opt Soc Am B 1996;13:481.
[52] Valeur B, Pouget J, Bourson J. J Phys Chem 1992;96:6545.
[53] Renouard T, Fallahpour RA, Nazeeruddin MK, Humphry-Baker R, Gorelsky SI, Lever ABP, et al. Inorg Chem 2002;41:367.
[54] Katan C, Terenziani F, Mongin O, Werts MHV, Porrès L, Pons T, et al. J Phys Chem A 2005;109:3024.